



Enhanced Photovoltaic Efficiency of Dye Sensitized Solar Cell by Few Layered Graphene Sheet Decked with SnO₂ Nanoparticles as a Photoanode

Satish Bykkam, K. Venkateswara Rao*, Ch. Shilpa Chakra

Nano Electronics Laboratory, Centre for Nano Science & Technology, Institute of Science & Technology, Jawaharlal Nehru Technological University, Hyderabad – 500 085, Telangana State, India.

ARTICLE DETAILS

Article history:

Received 25 May 2016

Accepted 09 June 2016

Available online 09 July 2016

Keywords:

Few Layered Graphene (FLG)

Photoanode

FLG/SnO₂ Nanocomposite

Dye Sensitized Solar Cell

ABSTRACT

In the current research work, the dye sensitized solar cell (DSSC) were fabricated by Few Layered Graphene (FLG) / SnO₂ nanocomposite used as a photoanode. FLG Weight (wt%) was varied from 1.0 % to 3.0 wt% with an interval of 1.0 wt% and investigated the effect of FLG wt% on their power conversion efficiency (η). The X-ray Diffraction (XRD) pattern confirmed the presence of FLG and SnO₂ nanoparticles (NPs) in FLG/ SnO₂ nanocomposites. High Resolution Transmission Electron Microscopy (HRTEM) shows that the nano sized SnO₂ particles are highly decked on FLG sheet. Based on the results obtained from UV-Visible Diffuse Reflectance Spectra (UV-DRS), the band gap of Pure SnO₂ NPs and FLG (1.0, 2.0 and 3.0 wt%)/SnO₂ nanocomposites are found to be \sim 4.239, 4.237, 4.210 and 4.172 eV respectively. Compared to Pure SnO₂ NPs, the FLG (1.0 wt%) / SnO₂ nanocomposite photoanode (η) was enhanced to 3.02 % with N719 dye under AM 1.5G, 100 mW/m² of solar simulator.

1. Introduction

In recent years, increasing global concerns about energy and the environment, more emphasis is being given to the development of economical and easily available alternative renewable energy sources as compared to non-renewable energy production and one of the most capable alternatives to the already existing conventional solar cells which uses renewable energy sources in the DSSC. DSSC have drawn great attention in photovoltaic's due to their ease of manufacturing relatively high efficiency, cost effective method and suitability for various applications [1-6]. In DSSC, dye plays a significant performance in harvesting solar light and converting solar energy into electrical energy [7,8]. In Fig. 1, DSSC Shows sandwich configuration which contains dye sensitized TiO₂ photo anode, I⁻/I³⁻ redox coupled electrolyte and a counter electrode coated with Pt [9].

In the present study, FLG used as a DSSC electrode in order to absorb maximum sunlight and also to efficiently increase the release of captured electrons from dye molecules to the external surface of the semiconductor films. Graphene is a new carbon based material in the field of nano science and technology, due to its excellent electrical, mechanical, and optical properties [10-12]. Graphene is one of the allotrope of carbon, looks like a honeycombed structured and each carbon atom is associated with bond length of 0.142 nm [13-15]. It has few certain features like high transparency and conductivity with low resistance of 106 Ω cm/sheet that makes an excellent feature for photovoltaic devices such as solar cells. Further, at room temperature, it shows highly excessive electron mobility, beyond 15,000 cm²/Vs. Based on these properties, recently garphehene has been applied to solar cell applications.

Tin oxide (SnO₂) is one of the semiconductor with wide band gap material, it has high permittivity and higher transparency which makes it suitable for DSSC photoanode. Its higher electron mobility (\sim 200 cm²V⁻¹S⁻¹) and long term stability when compared to TiO₂ (\sim 1 cm²V⁻¹S⁻¹) signifies the faster transport of electrons from photoanode. Diverse morphologies of SnO₂ have been used and tested for light harvesting and electron transport related to the open circuit (Voc) in devices. [16-18]. Recently, new structures (hollow spheres and octahedron) of SnO₂ have shown higher photovoltaic performance. The greater photovoltaic performance

of SnO₂ NPs is due to better electron transport properties and light scattering efficiency [19-20].

The present work, investigation of the photovoltaic performance based on FLG/SnO₂ nanocomposite photoanode for DSSC application. The introduction of FLG into photoanode used as a working electrode significantly, which is influencing the performances of DSSC. In addition, the effect of FLG on the DSSC parameters such as photo current density (Jsc), open circuit voltage (Voc), fill factor (FF) and power conversion efficiency (η) were investigated.

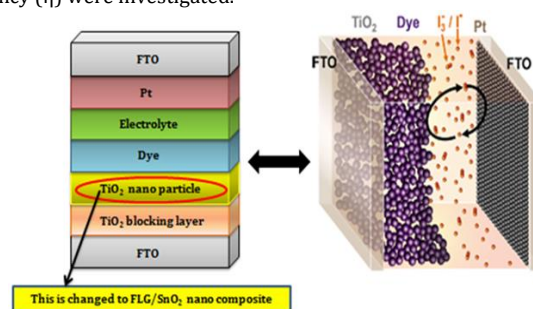


Fig. 1 Cell assembly Configuration of Dye Sensitized Solar Cell (DSSC).

2. Experimental Method

2.1 Preparation of FLG/SnO₂ Nanocomposite Photoanode

The preparation of the SnO₂ NPs paste and FLG/SnO₂ nanocomposite paste as a photoanode was schematically shown in Fig. 2. This study consists of two parts. In the first part, 2.0 g of SnO₂ nanopowder was dissolved in 20 mL of ethanol and subjected to ultrasonication bath for 30 min. After that the solution was transformed to a porcelain mortar and pestle and mixed with ethanol as a dispersing agent. Further, the paste was diluted by 1 mL PEG (MW 10000), which controls the viscosity of the paste. Finally few drops of detergent (Triton X-100) were added. In the second part, to obtain FLG/SnO₂ nanocomposite paste at different weight percentage of FLG (containing 1.0, 2.0 and 3.0 wt%), is prepared by Sacco et al [21] method. Briefly, FLG/SnO₂ nano composite powder also dissolved in ethanol and subjected to ultrasonication bath for 30 min, to form a stable colloidal dispersion was followed by in the same above method.

*Corresponding Author

Email Address: kalagadda2003@jntuh.ac.in (K. Venkateswara Rao)

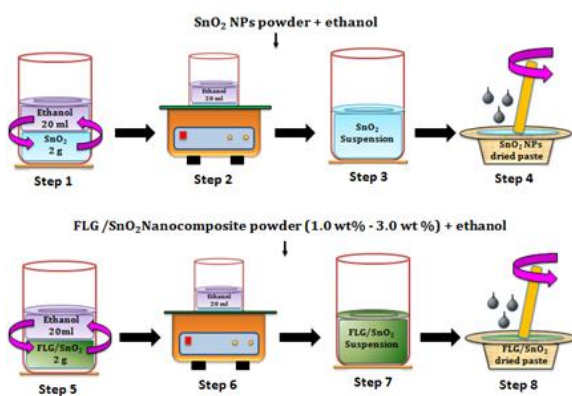


Fig. 2 Photoanode preparation of SnO₂ NPs and FLG/SnO₂ nanocomposite

2.2 Fabrication of DSSC

In Fig. 3 shows the fabrication of photoanode (working electrode) for DSSC, transparent conducting Fluorine-doped tin oxide (FTO)-coated glass substrates purchased from (sheet resistance = 9 Ohms/sq, and >80% transmittance in the visible region) were used. The FTO substrates were cleaned by ultrasonication in de-ionized water, acetone, and isopropyl alcohol for 15 min before use. By the Doctor blade technique, each FLG/SnO₂ nano composite paste were coated on a FTO glass substrate and labeled a to c (1.0, 2.0 and 3.0 wt% of FLG/SnO₂). For comparison, a reference photoanode exploiting the pure SnO₂ paste without FLG inclusion was fabricated with the same procedure. Then, the film were annealed at 450 °C for 1 hour, then cooled to 35 °C and immersed into the N719 (Ditetra-butylammonium bis(isothiocyanato) bis(2,2'-bipyridyl 4,4' dicarboxylato) ruthenium (II)) dye solution with a concentration of 0.5×10^{-3} M in ethanol for 24 hours. The organic solvent based liquid electrolyte was prepared from the solution of 0.6 M dimethylpropylimidazolium iodide, 0.1 M of iodine, 0.5 M tert-butylpyridine, and 0.1 M of lithium iodide in 3-methoxyacetonitrile. Platinum (Pt) sputtered FTO was used here as the counter electrode. The above two electrodes (working and counter) were assembled into a sandwich type cell using clamps. A drop of electrolyte was added to fill the space between two electrodes with a micro pipette. The assembled cell active area was 0.25 cm². The contact of the electrode was made using a silver paste.

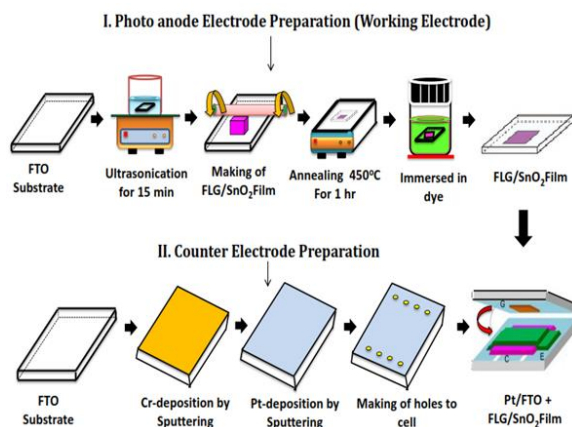


Fig. 3 Schematic Diagram of Devices Fabrication for DSSC

2.3 Characterization and Measurements

The crystal structure and morphology of prepared samples were characterized by X-ray diffraction (XRD, Model No: Bruker D8 advanced) and High resolution transmission electron microscopy (HR-TEM, Model No: JEOLJEM-200CX). The absorption spectra of the working photoanodes were recorded using Ultraviolet-Visible Diffuse Reflectance Spectrophotometer (UV-DRS, Model No: JASCO V-670). The photo current density- voltage (J-V) characteristics of cells were measured under solar illumination condition (100 mW/cm², AM 1.5G) using Oriol Class 3A solar simulator with Keithley 2440 source meter.

3. Results and Discussion

3.1 X-Ray Diffraction and HRTEM Analysis

The XRD patterns of the Pure SnO₂ NPs and FLG (1.0, 2.0 and 3.0 wt%)/SnO₂ nanocomposites are shown in Fig. 4. The calcination temperature at 600 °C for 4 hrs, the FLG/SnO₂ nanocomposite exhibited a tetragonal structure. The tetragonal structure showed 20 peaks at 26.8°, 33.9°, 37.9°, 51.8°, 54.8°, 57.7°, 61.8°, 64.8°, 66.0°, 71.2° and 78.6°, the corresponding to basal spacing (d₁₀₀), (d₁₀₁), (d₂₀₀), (d₂₁₁), (d₂₂₀), (d₀₂₀), (d₃₁₁), (d₁₁₂), (d₃₀₁), (d₂₀₂) and (d₃₂₁), planes respectively. The intensity of the planes decreased with an increase in the FLG weight percentage compared to Pure SnO₂ NPs. Using Scherrer's equation, $t = 0.9\lambda/\beta\cos\theta$, was used to calculate the crystalline size, where λ is the wavelength of the incident X-rays, β is full width half maximum (FWHM) height in radians and θ is the diffraction angle. The average crystalline size is found to be 28, 26, 24 and 22 nm for SnO₂ NPs and FLG (1.0, 2.0 and 3.0 wt%)/SnO₂ nanocomposites respectively. The characteristic (002) peaks of FLG at 26.2° is difficult to identify in all the FLG/SnO₂ nanocomposites, which may be because the FLG peaks weak and overlap with the (110) peak of pure SnO₂ NPs (26.8°).

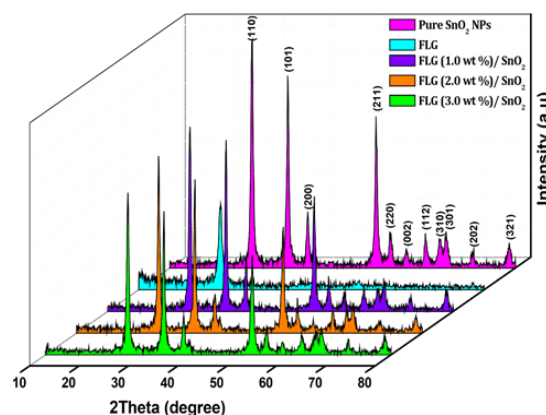


Fig. 4 XRD pattern of Pure SnO₂ NPs and FLG (1.0, 2.0 and 3.0 wt%)/SnO₂ nanocomposites

The HRTEM images of pure SnO₂ NPs and different weight percentage of FLG (1.0, 2.0 and 3.0 wt%)/SnO₂ nanocomposites are shown in Fig. 5. A relatively uniform spherical shaped particles with size around 20 ± 0.09 nm was observed in the Pure SnO₂ NPs which is shown in Fig. 5 (a-c). When FLG weight percentage added to the Pure SnO₂ NPs, they were stably dispersed and evenly distributed over the surface of the FLG sheet (Figs. 5d and e). Moreover, there are no free SnO₂ NPs observed beyond the FLG sheet as shown in Fig. 5f. The results show that FLG sheet is decked with SnO₂ NPs.

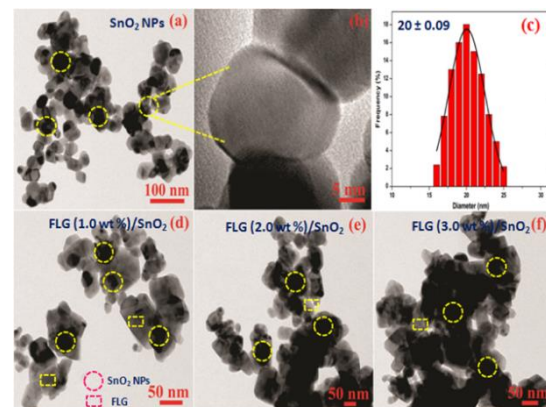


Fig. 5 HRTEM images of (a, b) Pure SnO₂ NPs (c) Particle size histogram of pure SnO₂ NPs (d) FLG (1.0 wt%)/SnO₂ (e) FLG (2.0 wt%)/SnO₂ (f) FLG (3.0 wt%)/SnO₂ nanocomposites

3.2 UV-DRS Analysis

Fig. 6 shows UV-DRS absorption spectra of the Pure SnO₂ NPs and FLG (1.0, 2.0 and 3.0 wt%)/SnO₂ nanocomposites. The tetragonal structure of SnO₂ NPs absorption peak is observed at 294 nm. In the spectra of FLG (1.0, 2.0 and 3.0 wt%)/SnO₂ nanocomposites the absorption peaks were slightly shifted to a longer wavelength compared to pure SnO₂ NPs. The absorption coefficient is presented by the following equation, defined as the Tauc law [22]: $(\alpha h\nu)^2 = \beta (h\nu - E_g)$ where E_g is the Tauc optical band gap, $\alpha = 2.303 A/d$ (A : optical density and d : thickness of the sample), β is constant.

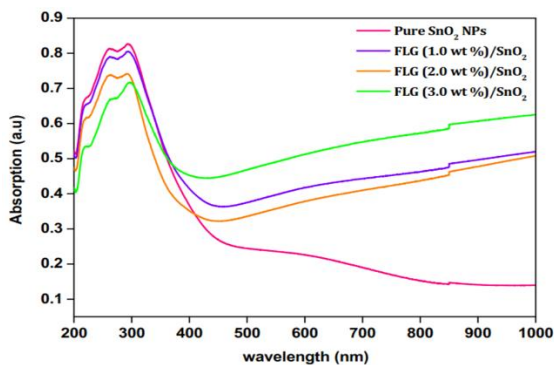


Fig. 6 Optical absorption spectra of Pure SnO₂ NPs and FLG (1.0, 2.0 and 3.0 wt%)/SnO₂ nanocomposites

The plot of $(\alpha h\nu)^2$ Vs $h\nu$ of Pure SnO₂ NPs and FLG/SnO₂ nanocomposites are shown in Fig. 7. The intercept of the abscissa axis with the full line of the $(\alpha h\nu)^2$ Vs $h\nu$ plot permits the calculation of the optical band gap. The obtained band gap of Pure SnO₂ NPs and FLG (1.0, 2.0 and 3.0 wt%)/SnO₂ nanocomposites are listed in Table 1. The FLG plays an important role in the performance of DSSC, electron accepting and donating under the light absorption. Here band gap of FLG tuned by introducing SnO₂ particles on the graphene sheets has proved.

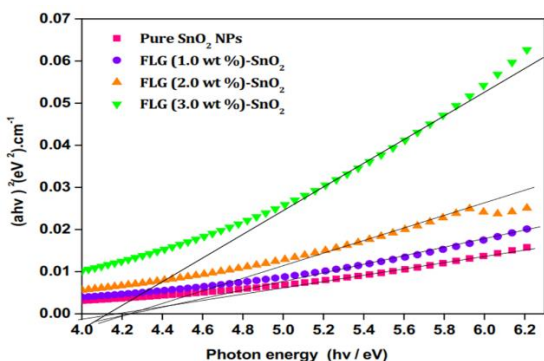


Fig. 7 Plot of $(\alpha h\nu)^2$ Vs $h\nu$ of Pure SnO₂ NPs and FLG(1.0,2.0 and 3.0 wt%)/SnO₂ nanocomposites

Table 1 Energy band gap values of Pure SnO₂ NPs and FLG (1.0, 2.0 and 3.0 wt%)/SnO₂ nanocomposites

	SnO ₂ NPs	FLG (1.0 wt%) / SnO ₂	FLG(2.0 wt%) / SnO ₂	FLG(3.0 wt%) / SnO ₂
Band Gap (eV)	4.239	4.237	4.210	4.172

3.3 Photovoltaic Performances of DSSC

The current-voltages (I-V) components of N719 dye based on pure SnO₂ NPs and FLG/SnO₂ nanocomposite photoanodes are shown in Fig. 8. Based on the I-V characteristics of the DSSC, the Fill Factor (FF) was calculated using the relation [23].

$$FF = \frac{(I_{max} \cdot V_{max})}{(I_{sc} \cdot V_{oc})} \quad (1)$$

where, I_{max} and V_{max} are the photo current and photo voltage for maximum power output, and I_{sc} and V_{oc} are the short-circuit photo current and open-circuit photo voltage, respectively. The η was calculated using the following expression [24].

$$\eta (\%) = \frac{(V_{opt} \cdot I_{opt})}{(P_{in})} \times 100 = \frac{(V_{oc} \cdot I_{sc} \cdot FF)}{(P_{in})} \times 100 \quad (2)$$

where V_{opt} and I_{opt} are the optimal voltage and current respectively. P_{in} is the power of incident light.

The photovoltaic parameters V_{oc} , J_{sc} , FF and η are given in Table 2. DSSC assembled with a Pure SnO₂ NPs has V_{oc} of 0.62 V and J_{sc} of 6.64 mA/cm². The η was 1.93% of the Pure SnO₂ NPs photoanode, but increased to 3.02% in the DSSC made from FLG (1.0 wt%)/SnO₂ nanocomposite photoanode, with a V_{oc} of 0.51 V and J_{sc} of 12.21 mA/cm². The values are decreased for corresponding of FLG (2.0 wt%)/SnO₂ (0.51 V, 5.87 mA/cm² and 1.44%) and FLG (3.0 wt%)/SnO₂ (0.44 V, 4.22 mA/cm² and 1.00%) nanocomposite photoanode.

On the other hand, when FLG weight percentage was further increased from 2.0 to 3.0 wt%, the corresponding J_{sc} started to decrease from 5.87 mA/cm² to 4.22 mA/cm² and η decreased from 1.41% to 1.00%. This could be due to the following reasons: (a) The increase in wt% of FLG, which is reduced light absorption and also decreased the number of photo excited electrons on the surface of SnO₂ NPs film; (b) Increased FLG wt% in SnO₂ NPs film, the surface resistance and film thickness increased; (c) At higher wt% of FLG (2.0 and 3.0 wt %) the corresponding η values are slightly decreased due to less generation of electron-hole pair. Generally, the higher weight percentage of FLG in composites, the dye molecules absorb less sunlight.

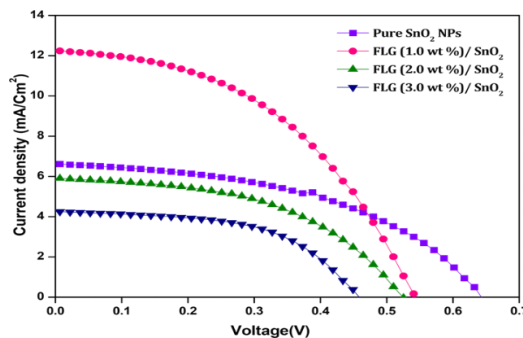


Fig. 8 J-V curves of pure SnO₂ and different FLG (1.0, 2.0 and 3.0 wt%)/SnO₂ photoanode based DSSC

Table 2 Photovoltaic (parameters) of the DSSC based on pure SnO₂ NPs and different FLG (1.0, 2.0 and 3.0 wt%) /SnO₂ photoanodes

Photoanodes	V_{oc} (V)	J_{sc} (mA/cm ²)	FF (%)	η (%)
SnO ₂ NPs	0.62	6.64	46.6	1.93
FLG (1.0 wt %) / SnO ₂	0.54	12.21	45.6	3.02
FLG (2.0 wt %) / SnO ₂	0.51	5.87	48.2	1.44
FLG (3.0 wt %) / SnO ₂	0.44	4.22	53.8	1.00

3.4 Effect of FLG wt% on DSSC Parameters

By increasing the contents of FLG involved in SnO₂ film, in the range of 1.0, 2.0 and 3.0 wt% among these, the V_{oc} values of 1.0 wt% FLG was obtained higher than the 2.0 and 3.0 wt% of the FLG. The values are slightly decreased as shown in Fig. 9a. By the same way, these values of J_{sc} and η also increased with the FLG content, until a decrease when the FLG content up to 3 wt% as shown in Figs. 9(b-c). This might be high FLG content involved SnO₂ film increased the surface resistance of the SnO₂ and the further increase in film thickness. In the case, by increasing the FLG content for improvement of efficiency is not substantial, but the 1.0 wt% of FLG involved in SnO₂ film improves the current and all cell parameters by suppressing the electron recombination.

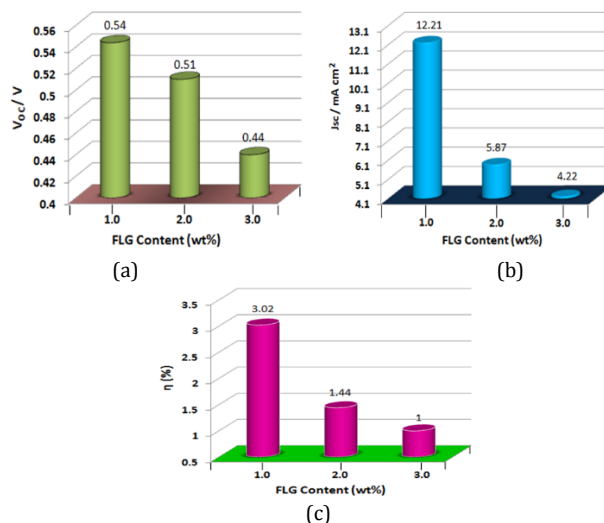


Fig. 9 Standard DSSC with SnO₂ containing FLG (1.0, 2.0 and 3.0 wt%) for photo current density-voltage characteristics (a) Voc (b) J_{sc} and (c) η %

Fig. 10 shows schematically energy level diagram of N719 dye using FLG/SnO₂ nanocomposite photoanode. The step wise energy level of N719, SnO₂, FLG and FTO is beneficial for electron to transport from lowest unoccupied molecular orbital (LUMO) of N719 dye to FTO a substrate. a

suitable ratio of FLG bridges acts as an electron transfer channel, to carry the generated electron rapidly without any obstruction. According to the results, we observed FLG effects a significant development in the performance of DSSC in our study.

For further performance of DSSC, FLG can be considered in two main aspects: (1) Increased dye adsorption, by introducing of FLG and tuning of the band gap of FLG by using metal oxides provides a more active site for absorption of dye molecules, which draws in more light and contributes to more photo induced electron induced from the excited state (LUMO) of dye into the conduction band of SnO₂ and (2) Significant longer electron lifetime, which high aspect ratio, FLG sheet has very low conductive percolation threshold, much less than 3.0 wt%. In our work, with 1.0 wt% contained; FLG was dispersed uniformly in the matrix of SnO₂ to form the effective and continuous 2D conductive network. The excited possible electrons move from the conduction band of SnO₂ to graphene, as shown in Fig. 10. Then, the electron transfer through the graphene sheet and are collected by the FTO substrate. In traditional SnO₂ photoanode, photo induced electrons have the capability to transfer through the film, which is few micrometers thick before reaching the FTO substrate, and have more possibilities to be recombined by hole. In our work FLG/SnO₂ nanocomposite photoanode, FLG has work function similar to the FTO [26] it acts more like many persistent current collectors penetrating into the SnO₂ matrix and the electrons will be rapidly captured or collected before recombination.

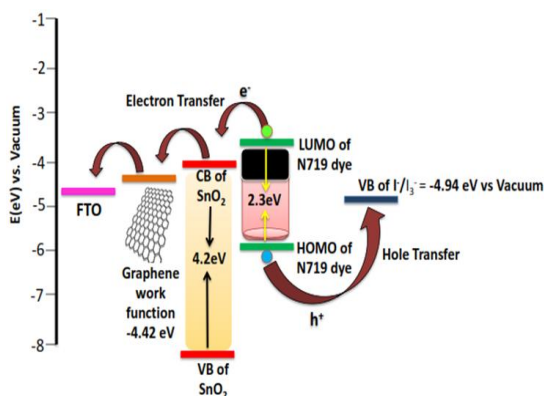


Fig. 10 Schematic energy level diagram of N719 dye using FLG/SnO₂ photoanode. The Fermi level of SnO₂, graphene and redox (I⁻/I₃⁻) are set a -4.00 [24], -4.22 [25], -4.94 [26].

4. Conclusion

Successfully prepared pure SnO₂ NPs and different weight percentage of FLG (1.0, 2.0 and 3.0 wt%)/SnO₂ nanocomposites pastes to fabricate photoanodes for DSSC Application. A noteworthy improvement (3.02%) in power conversion efficiency (η) was achieved in DSSC using FLG (1.0 wt%)/SnO₂ nanocomposite photoanode as compared to another based on Pure SnO₂ NPs under A.M 1.5G solar simulated. The results, verifies that suitable ratio of (1.0 wt%) FLG in SnO₂ performs the role of blocking layer to suppress the back electron-hole recombination in DSSC and thus enhance the power conversion efficiency. However, higher wt% of the FLG loading beyond the optimal wt% can cause the decrease of the efficiency due to the light shielding of the FLG.

Acknowledgements

Author sincerely thanks to University Grant Commission (UGC-Government of India) for financial support through "Rajiv Gandhi National Fellowship" (File no.F1-17.1/2012-13/RGNF-2012-13-SC-AND-30114). Centre for Energy Studies (CES), Plasmonic Solar cell Laboratory, IITD-

Delhi for providing necessary facilities to carry out the present research work. We wish to give special thanks to Mr. T. Eshwar for helping in DSSC application. And also thanks to Mr. Ramana Babu & Mr. A.Uppalaiah, for help in UV-DRS at Central Analytical Laboratory, Bits-Pilani Hyderabad Campus.

References

- [1] J.B. O'Regan, M. Gratzel, A low-cost,high-efficiency solar cell based on dye-sensitized colloidal TiO₂ films, *Nature* 353 (1991) 737-740.
- [2] M.D.K. Nazeeruddin, R. Humphry-Baker, P. Liska, M. Gratzel, Investigation of sensitizer adsorption and the influence of protons on current and voltage of a dye-sensitized nanocrystalline TiO₂ solar cell, *J. Phys. Chem. B* 107 (2003) 8981-8987.
- [3] J. Jiu, S. Isoda, F. Wang, M. Adachi, Dye sensitized solar cells based on a single crystalline TiO₂ nanorod film, *J. Phys. Chem. B* 110 (2006) 2087-2092.
- [4] A. Hagfeldt, M. Gratzel, Molecular photovoltaics, *Acc. Chem. Res.* 33 (2000) 269-277.
- [5] A. Hagfeldt, M. Gratzel, Light induced redox reactions in nanocrystalline systems, *Chem. Rev.* 95 (1995) 49-68.
- [6] M. Gratzel, Review article photo electrochemical cells, *Nature* 414 (2001) 338-344.
- [7] J. Gong, J. Linga, K. Sumathy, Review on dye-sensitized solar cells (DSSCs): Fundamental concept and novel materials, *Renew. Sustain. Energy Rev.* 16 (2012) 5848-5860.
- [8] S. Lin, K.C. Lee, J.L. Wu, J. Yi Wu, Plasmon-enhanced photo current in dye-sensitized solar cells, *Solar Energy* 86 (2012) 2600-2605.
- [9] J. Sheng, L.H. Hu, S.Y. Xu, W.Q. Liu, L. Mo, H.J. Tian, S.Y. Dai, Characteristics of dye sensitized solar cells based on the TiO₂ nanotube/nano particle composite electrodes, *J. Mater. Chem.* 21 (2011) 5457-5463.
- [10] K.S. Novoselov, A.K. Gemi, S.V. Marozov, D. Jiang, Y. Zhang, S.V. Dubonos, et al, Electrical field effect in atomically thin carbon films, *J. Sci.* 306 (2004) 666-669.
- [11] H. Chen, M.B. Muller, K.J. Gilmore, Mechanically strong, electrically conductive and biocompatible graphene paper, *Adv. Mater.* 20 (2008) 3557-3561.
- [12] A.K. Gemi, K.S. Novoselov, The rise graphene, *Nature Mater.* 6 (2007) 183-191.
- [13] S. Stankovich, D.A. Dikin, R.D. Piner, K.A. Kohlhaas, A. Kleinhammes, Y. Jia, et al, Synthesis of graphene-based nanosheets via chemical reduction of exfoliated graphite oxide, *Carbon* 45 (2007) 1558-1565.
- [14] X. Wang, L. Zhi, K. Mullen, Transparent conductive graphene electrodes for dye-sensitized solar cells, *Nano Lett.* 8 (2008) 323-327.
- [15] K. Zhou, Y. Zju, X. Yang, C. Li, One-pot preparation of graphene/Fe₃O₄ composites by a solvothermal reaction, *New J. Chem.* 34 (2010) 2950-2955.
- [16] S. Gubba, V. Chakrapani, V. Kumar, M.K. Sunkara, Band edge engineering hybrid structures for dye sensitized solar cells based on SnO₂ nano wires, *Adv. Funct. Matter.* 18 (2008) 2411-2418.
- [17] J. Qian, P. Liu, Y. Xiao, Y. Jiang, Y. Cao, X. Ai, H. Yang, TiO₂ coated multilayered SnO₂ hollow micro spheres for dye sensitized solar cells, *Adv. Matter.* 21 (2009) 3663-3667.
- [18] C. He, B. Lei, Y. Wang, C. Su, Y. Fang, D. Kuang, Sonochemical preparation of hierarchical ZnO hollow sphere for efficient dye sensitized solar cells, *Chem. Eur. J.* 16 (2012) 8757-8716.
- [19] H. Zhang, Y. Han, X. Liu, P. Liu, H. Yu, S. Z hang, et al, Anatase TiO₂ microspheres with exposed mirror like plane facets for high performance dye sensitized solar cells, *Chem. Commun.* 46 (2012) 8395-8397.
- [20] Y. Wang, W. Yang, W. Shi, Preparation and characterization of Anatase TiO₂ nanosheets based microspheres for dye sensitized, sensitized solar cells, *Indus. Engg. Chem. Res.* 50 (2011) 11982-11987.
- [21] A. Sacco, S. Porro, A. Lamberti, M. Gerosa, M. Castellino, A. Chiodoni, S. Bianco, Investigation of transport and recombination properties in graphene/titanium dioxide nano composite for dye sensitized solar cell photo anodes, *Electrochem. Acta* 131 (2014) 154-159.
- [22] J. Tauc, Amorphous and liquid semiconductors, Plenum Press, New York, 1974.
- [23] K. Wongcharee, V. Meeyoo, S. Chavadei, Dye-sensitized solar cell using natural dyes extracted from rosella and blue pea flowers, *Sol. Ener. Mater. Sol. Cells* 91 (2007) 566-571.
- [24] A. Chowdhuri, D. Haridas, K. Sreenivas, V. Gupta, Mechanism of trace level H₂S gas sensing using Rf sputtered SnO₂ thin films with CuO catalytic overlayer, *Inter. J. Smart Sens. Intelligent Sys.* 2 (2009) 540-548.
- [25] R. Czrew, B. Foley, D. Tekleab, A. Rubio, P. Ajayan, D. Carroll, Substrate-interface interaction between carbon nanotubes and the supporting substrate, *Phys. Rev. B* 66 (2002) 334081-334084.
- [26] A. Andersson, N. Johansson, P. Broms, N. Yu, D. Lupo, W.R. Salaneck, Fluorine tin oxide as an alternative to indium tin oxide in polymer leds, *Adv. Mater.* 10 (1998) 859-863.